COHERENT RADAR IMAGING AND THE EFFECTS OF REFLECTIVITY FIELD VARIATIONS AND BIOLOGICAL CLUTTER

B. L. Cheong[1], M. W. Hoffman[1], R. D. Palmer[1], H. Tong[1], V. Tellabati[1]
S. J. Frasier[2] and F. J. López-Dekker[2]

[1]University of Nebraska-Lincoln, U.S.A. [2]University of Massachusetts, Amherst, U.S.A.

1. INTRODUCTION

This brief article highlights the progress of simulation studies of the Turbulent Eddy Profiler (TEP)[1] using a standard configuration and a new proposed array configuration. Variations on the reflectivity field were found to have systematic bias on the radar imaging process using the traditional Fourier method. By using the adaptive Capon method, the bias from the reflectivity variations were significantly reduced. In addition, a study of the effects of biological clutter in the antenna sidelobes was conducted. Most cases of biological clutter occur from targets in the sidelobes of the antenna.[2] With a subtle change to the TEP array, it is possible to use the Capon beamforming method to virtually eliminate the effects of biological targets in the antenna sidelobes on wind field estimates. It should be noted that the proposed array configuration does not have this beneficial effect using standard Fourier beamforming.

2. EFFECTS OF REFLECTIVITY VARIATIONS ON RADAR IMAGING

One of the main goals of this experiment is to study the variations of the reflectivity distribution on the imaging process. The numerical simulation presented uses a modified version of the method of *Holdsworth and Reid*[3] with a simple reflectivity pattern shown in Figure 1. A

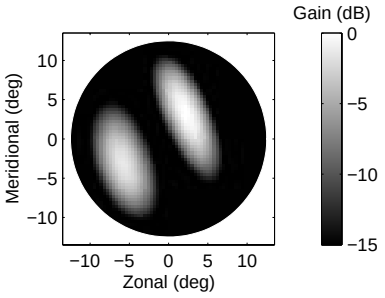

Figure 1. *Model reflectivity used in the simulation is a map with two bivariate Gaussian functions centered at (2°, 4°) and (-6°, -4°). A uniform horizontal wind from* 25° *at 25* ms^{-1} *and a turbulent wind field of* ± 1 ms^{-1} *were used in the simulation.*

uniform horizontal wind (25 ms^{-1} at 45° azimuth) and a turbulent wind field of $\pm$ 1 ms^{-1} across the entire imaging region were used in this simulation. By using radar imaging with TEP, it is possible to reconstruct the reflectivity and wind fields within the beam of the radar.

The left panel of Figure 2 shows two reconstructed images using Fourier and Capon beamforming.[4] An interesting feature is observed near the valley between the two reflectivity peaks. Note the systematic over and under estimation compared to the known actual horizontal velocity indicated by the single arrow in the upper right corner of each frame. Variations in the reflectivity pattern along the direction of the wind are accompanied by either systematic increases, decreases, or rotations in horizontal wind vector estimates. It appears that the variation is more significant in the case of the Fourier estimators than it is for the Capon estimates. The right panel of Figure 2 illustrates the effects of reflectivity variations on the estimates of radial velocity and Figure 3 illustrates the deterministic bias on the radial velocity estimates based on our theoretical argument.

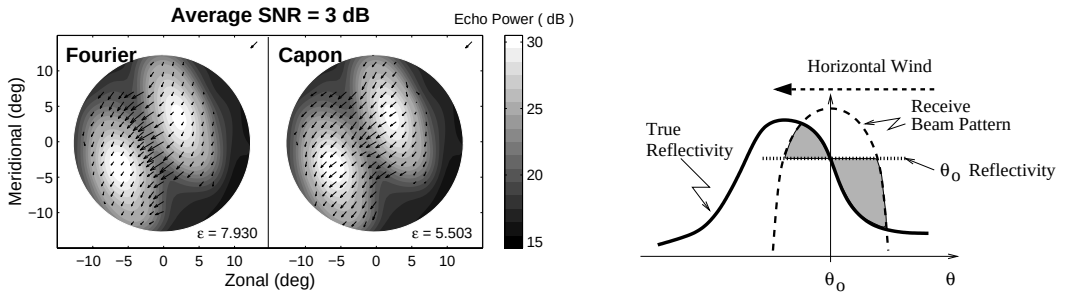

Figure 2. *The left panel shows the images obtained after processing the signals from the simulation. The datasets are processed with both the Fourier and Capon methods. The right panel is a graphical illustration of the effects of reflectivity variation along the wind directions. The shaded regions show the weighting effects of radial velocities. In this example, the radial velocities are under and over weighted on the right and left of θ_o, respectively. This weighting depends on the reflectivity variations, the wind direction and the antenna beam pattern and contritubes a deterministic bias to the radial velocity estimates.*

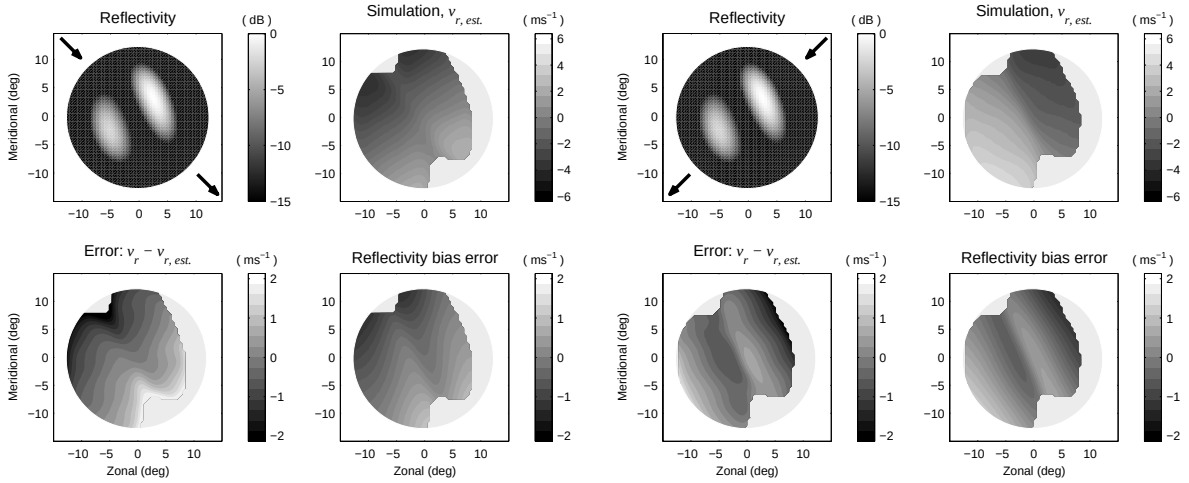

Figure 3. *These plots show the effects of reflectivity variations for two cases with different wind directions. The upper left panel is the true reflectivity with horizontal wind as indicated. The upper right panel is the radial velocity estimate. The lower two panels show the radial velocity estimate error (left) and the predicted bias obtained using the known wind field, the known reflectivity, and the Fourier beampattern.*

3. OPTIMAL SUBARRAY DESIGN

A simple Gaussian reflectivity field pattern is used in this part of the experiment. The main goal of this experiment is to address the bird clutter rejection issue; the model reflectivity is irrelevant. For the first few frames of the simulation, the bird moves through the main lobe of the antenna. Subsequently, the bird moves through a grating lobe. No known method is available to eliminate the bird echo from the main lobe. However, the proposed array configuration shown in Figure 4 (left panel) can significantly reduce the effect of the bird as it progresses through the grating lobes. The quality of the wind field estimates using the original TEP array and proposed array configuration will be compared. Initially, the three subarrays were designed to allow spatial smoothing to mitigate the clutter. However, it was later discovered that imaging using the Capon beamforming method[4] outperformed the spatial averaging method. The results in this report show the performance of the newly configured array using the Capon beamforming method. A statistical search was performed in order to find the optimal array configuration. Figure 4 shows the new array configuration with three hexagonal subarrays and the array response of the system. The right panel shows the total beampattern of the system with nulls in the centers of each grating lobe allowing the mitigation of clutter effects.

One of the main goals of the TEP system is to estimate the three-dimensional wind field with high angular resolution. The proposed array configuration greatly benefits this goal by virtually eliminating the effects of grating lobe echoes in the wind field estimates. Figure 5

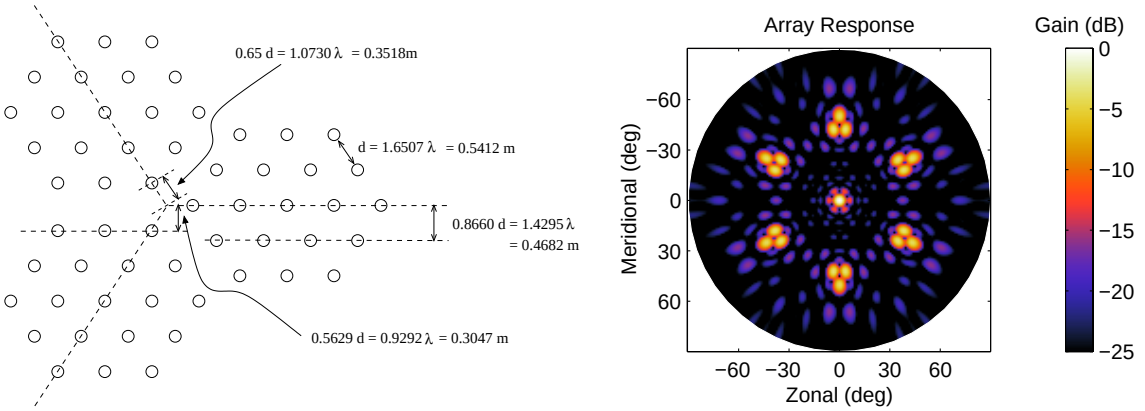

Figure 4. *The proposed TEP subarray array configuration. Subarrays are designed to mimic the original TEP configuration. Note that three subarrays are used which have a slightly different spacing from the original element spacing.*

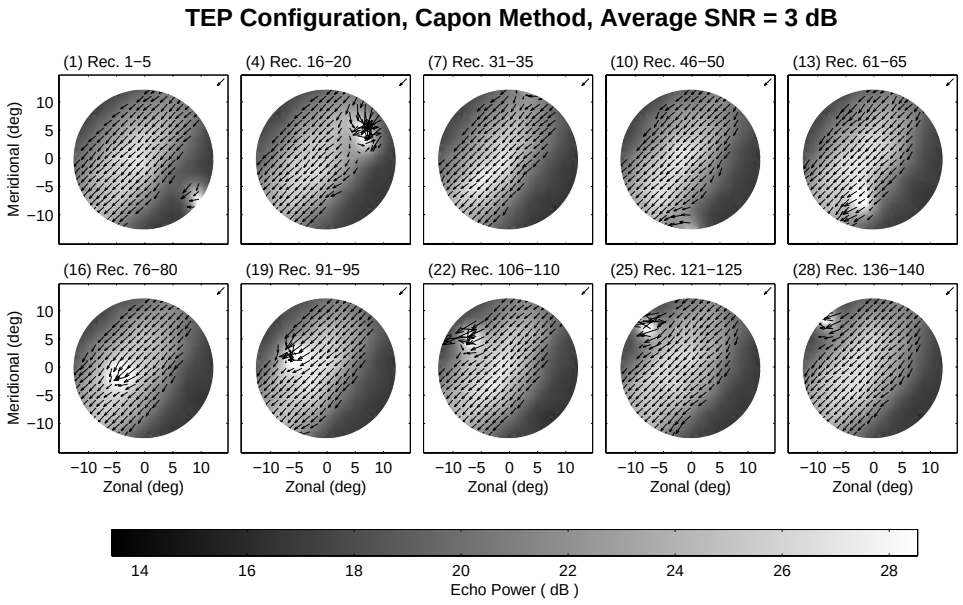

Figure 5. *A uniform wind field is simulated with original TEP array. This series of images show the power distribution obtained using Capon beamforming method with the original TEP array. Using the original TEP configuration, it can be seen that there is a bird flying across the main imaged region in frames 1-7. As the bird continues to fly, it passes through a grating lobe toward the north and is seen as an angularly aliased signal in the maps (frames 10-28).*

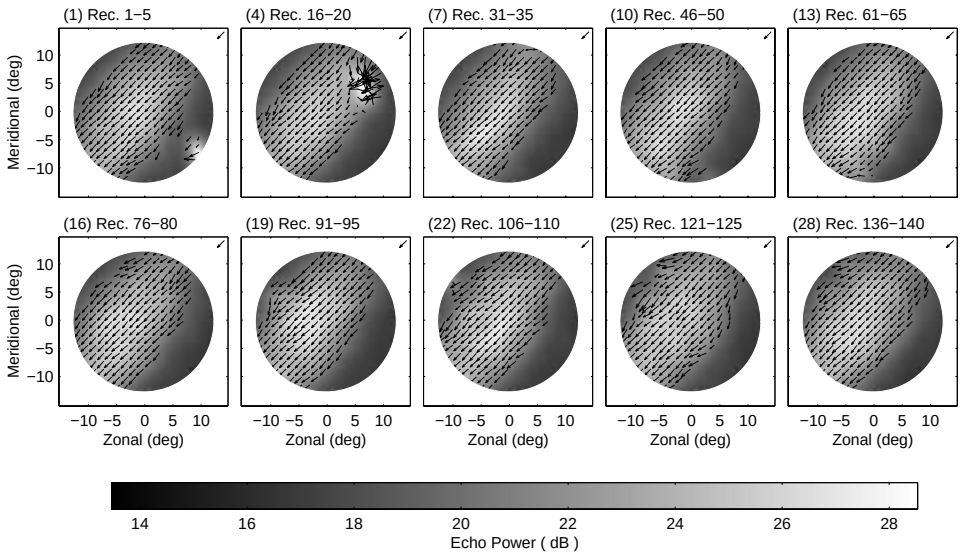

Figure 6. *Same as Figure 5, except using the proposed subarray configuration. As the bird flies through the main beam it is seen in the image (frames 1-7) as in the original TEP array configuration. However, as the bird passes through the grating lobe its returned power is significantly reduced and unique beampattern of the subarray configuration mitigates the interference of the bird clutter in the wind estimation procedure.*

shows a series of images of echo power and wind field estimates for a bird flying across the main imaging region using the original TEP array. As the bird continues, it flies across the grating lobe of the array and is seen as an aliased signal in the images and appears as a moving distortion in the wind field.

For the optimized array configuration, the results are significantly different and are provided in Figure 6. Note that the frame is indicated by the number in parenthesis. During frames 1-7, the bird flies across the main lobe and is seen as an ordinary scatterer with strong reflectivity. However, the grating lobe interference from the bird is significantly reduced in the subarray configuration providing a more accurate wind field map compared to the original TEP configuration. In frames 10-28, however, the bird echo is angularly aliased into the observed image. By using the proposed subarray configuration (refer to Figure 6), a strong returned signal can be seen as the bird moves across the main imaging area. However, during frames 10-28, the bird echo power is greatly reduced and is undetectable. The unique grating lobe structure, caused by the array design, produces significantly higher quality wind field images. Given the fact that a majority of bird echoes occur from sidelobe/grating lobe echoes, the proposed array design warrants further study and experimentation.

REFERENCES

1. J. B. Mead, G. Hopcraft, S. J. Frasier, B. D. Pollard, C. D. Cherry, D. H. Schaubert, and R. E. McIntosh, "A volume-imaging radar wind profiler for atmospheric boundary layer turbulence studies," *J. Atmos. Oceanic Technol.* **15**, pp. 849–859, 1998.
2. J. M. Wilczak, R. G. Strauch, F. M. Ralph, B. L. Weber, D. A. Merritt, J. R. Jordan, D. E. Wolfe, L. K. Lewis, D. B. Wuertz, J. E. Gaynor, S. A. McLaughlin, R. R. Rogers, A. C. Riddle, and T. S. Dye, "Contamination of wind profiler data by migrating birds: Characteristics of corrupted data and potential solutions," *J. Atmos. Oceanic Technol.* **12**, pp. 449–467, 1995.
3. D. A. Holdsworth and I. M. Reid, "A simple model of atmospheric radar backscatter: Description and application to the full correlation analysis of spaced antenna data," *Radio Sci.* **30**, pp. 1263–1280, 1995.
4. R. D. Palmer, S. Gopalam, T. Yu, and S. Fukao, "Coherent radar imaging using capon's method," *Radio Sci.* **33**, pp. 1585–1598, 1998.